ACTA ABP BIOCHIMICA POLONICA

Vol. 69, No 4/2022
795–804
https://doi.org/10.18388/abp.2020_6118

Regular paper

E2F1-induced long non-coding RNA MCF2L-AS1 modulates Cyclin D1 mRNA stability through ELAVL1 to induce Gefitinib resistance in non-small cell lung cancer

Kui Zhong Shan✉, Su Fang Yang, Yu Jiang Deng, Pei Yu Yue and Zhi Quan Du

Department of Pulmonary Nodule Center, The Second People's Hospital of Kunshan, Suzhou, China

Purpose: Gefitinib is a widely used therapeutic drug for non-small cell lung cancer (NSCLC), and its acquired resistance has become one of the barriers to the successful use of the drugs to treat NSCLC patients. Long non-coding RNA (lncRNA) has an essential role in developing cancer drug resistance. Hence, this study aimed to investigate the effect and modulatory mechanisms of lncRNA MCF2L-AS1 in Gefitinib resistance in NSCLC. Methods: IBEAS-2B and A549 cells and human NSCLC tissues were used. A549/GR cell line was constructed by continuous exposure to Gefitinib. Cell viability, apoptosis, migration, colony formation, and protein expression studies were done in transfected cells. Interactions of MCF2L-AS1, ELAVL1, and Cyclin D1 (CCND1 was also investigated. Results: In patients with Gefitinib-resistant NSCLC, MCF2L-AS1 and CCND1 were both up-regulated. Knockdown of MCF2L-AS1 reduced Gefitinib-resistant NSCLC cell progression, indicating that inhibition of MCF2L-AS1 restrained Gefitinib-resistant NSCLC. Mechanically, MCF2L-AS1 enhanced CCND1 mRNA stability *via* combining with ELAVL1, thereby elevating the resistance of NSCLC cells to Gefitinib. Moreover, E2F1 could transcriptionally up-regulate MCF2L-AS1. Conclusion: The results manifest that lncRNA MCF2L-AS1, as an oncogene of NSCLC, controls CCDN1 *via* ELAVL1 to drive the growth of NSCLC cells and Gefitinib resistance.

Keywords: Non-small cell lung cancer, Gefitinib, Drug resistance, Long non-coding RNA MCF2L-AS1, CCND1, ELAVL1

Received: 28 December, 2021; revised: 22 April, 2022; accepted: 27 April, 2022; available on-line: 18 October, 2022

✉e-mail: skzhong856@163.com
Acknowledgements of Financial Support: This study was supported in part by grants from the Kunshan Science and Technology Bureau Project (grant no. KS1905).
Abbreviations: CSCs, cancer stem cells; EGFR, Epidermal growth factor receptor; LC, lung cancer; lncRNA, long non-coding RNA; NSCLC, non-small cell lung cancer; RBPs, RNA binding proteins; TKI, EGFR-tyrosine kinase inhibitor

INTRODUCTION

Lung cancer (LC) is a malignant tumor with the highest morbidity and mortality worldwide and has extensive drug resistance (Wang *et al.*, 2020). Non-small cell lung cancer (NSCLC) is the major subtype of LC, taking up about 85–90% of all LC cases. Research advances have the diagnosis and treatment approaches to NSCLC. The currently used therapeutic methods include surgery, radiotherapy, chemotherapy, and targeted drug therapy. However, the prognosis of NSLC remains poor, with low survival rates.

Epidermal growth factor receptor (EGFR) is an oncogenic receptor tyrosine kinase that is crucial in establishing and spreading NSCLC. Gefitinib is a first-generation EGFR-tyrosine kinase inhibitor (TKI) that reversibly binds with the ATP cleft at the EGFR kinase domain, thus blocking EGFR auto-phosphorylation, hence effective in NSCLC (Kwon *et al.*, 2015). However, increased resistance to Gefitinib has been recently reported among NSCLC patients, resulting in treatment failure. Consequently, understanding the mechanisms of Gefitinib resistance to NSCLC is necessary to develop an effective therapy.

Several reports have confirmed the role of long non-coding RNA (lncRNA) in cancer drug resistance. According to the previous investigations, LINC01116 induces gefitinib resistance in NSCLC *via* controlling IFI44 while lncRNA UCA1 controls FOSL2 through competition with microRNA (miR)-143 to elevate Gefitinib resistance in NSCLC (Chen *et al.*, 2020). Further, lncRNA H19 has also been shown to contribute to the resistance of Gefitinib to LC (Lei *et al.*, 2018). A study reported that lncRNA MCF2L-AS1 drives colorectal cancer (CRC) progression through the miR-874-3p/FOXM1 axis (Zhang *et al.*, 2021). LncRNA MCF2L-AS1 up-regulates CCND1 through sponging miR-874-3p, thereby elevating the invasiveness of CRC (Huang *et al.*, 2021). LncRNA MCF2L-AS1 is enhanced in LC tissues and cells and drives NSCLC stem cell-like characteristics *via* down-regulating miR-873-5p (Ajani *et al.*, 2015). In the meantime, cancer stem cells (CSCs) have the ability of self-renewal and multi-lineage differentiation, which are linked with the occurrence, progression, metastasis, recurrence, and resistance of tumors to drugs (Li *et al.*, 2021). Nevertheless, no studies have reported the role of lncRNA MCF2L-AS1 in the resistance of Gefitinib to NSCLC.

LncRNA, being a latent modulator of various cellular processes, has several roles, including modulation of RNA binding proteins (RBPs), motivation of mRNA transcription, and post-transcriptional controlling through sponging miRNAs (Sana *et al.*, 2012). For instance, NHG12 binds with the RNA binding protein HuR, stabilizes YWHAZ, and accelerates the proliferation of gastric cancer (Zhang *et al.*, 2021). LncRNA TSLNC8 drives the growth and metastasis of pancreatic cancer through HUR-mediated CTNNB1 mRNA stability (Chai *et al.*, 2021). Meanwhile, HuR (ELAVL1) has been reported as the common RNA binding protein of lncRNA MCF2L-AS1 and CCND1. The previous investigation confirmed an increased ELAVL1 in NSCLC

tissues (Ni *et al*., 2020). Cyclin D1 (CCND1) is an essential molecule in the cell cycle transition from the G1 phase to the S phase, and it is elevated in numerous tumors. Linc00703 has been confirmed to inhibit NSCLC progression *via* repressing CCND1 (Sun *et al*., 2020), while LncRNA PCNA-AS1 enhances NSCLC cells proliferation *via* up-regulating CCND1 (Wu *et al*., 2020). The current study hypothesized that lncRNA MCF2L-AS1 might accelerate the stability of CCND1 mRNA *via* combining with ELAVL1 to elevate Gefitinib resistance in NSCLC.

MATERIALS AND METHODS

Ethical statement and clinical samples

The research approval was done by the Ethics Committee of the Second People's Hospital of Kunshan. Written consent was obtained from all the study participants. The NSCLC human samples were collected from 2016 to 2019. The samples were divided into the control group (not receiving Gefitinib treatment, n=10) and the Gefitinib resistant group (relapse after Gefitinib treatment, n=15, NSCLC patient tissues). The tissues were immediately frozen in liquid nitrogen and stored at –80°C for further experiments.

Cell culture and treatment

Normal human lung epithelial cells BEAS-2B cells and lung adenocarcinoma A549 cells were purchased from ATCC (Rockville, MD, USA). The cells were cultured in Dulbecco's Modified Eagle Medium (DMEM) with 10% fetal bovine serum (FBS; Invitrogen, Carlsbad, CA, USA), 100 U/mL penicillin, 100 μg/mL streptomycin. The medium was changed daily, and cells were harvested at the logarithmic growth phase for further experiments.

Gefitinib-resistant cell line establishment

Gefitinib-resistant cell line (A549/GR) was established as reported elsewhere (Rho *et al*., 2009). Briefly, the parental A549 cells were exposed to 5 μM Gefitinib (Santa Cruz Biotechnology, CA, USA) for 48 h in DMEM supplemented with 10% FBS. The cells were then washed and incubated in a drug-free medium until the surviving cells' population reached 80% confluence. Next, the surviving cells were continuously exposed to increasing Gefitinib dosages which were sequentially increased to 5, 10, 15, 20, 25, and 30 M (after every 2 months). The constructed resistant cell line was maintained by culturing in DMEM containing 30 M Gefitinib.

Cell transfection

The cells (2×10^5) were harvested in the logarithmic phase, plated in a 6-well culture plate, and grown to a confluence of 70%. The cells were later transfected using sh-MCF2L-AS1-1/MCF2L-AS1-2/ELAVL1/CCND1/E2F1, Oe-E2F1, sh-MCF2L-AS1 + Oe-CCND1, sh-E2F1 + Oe-MCF2L-AS1 and their corresponding negative controls (NCs) (all GenePharma Co. Ltd., Shanghai, China). The Lipofectamine 2000 transfection kit (11668-027, Invitrogen, USA) was used for the transfections following the manufacturer's instructions. After transfections, the cells were cultured for 24 h after which the media was changed, and the cells were cultured further.

Cell counting kit (CCK)-8 assay

Cells in the logarithmic phase were trypsinized for 2 min at 37°C to a single cell suspension. The cells were resuspended in 1 mL of complete media and counted. Next, a 100 μl suspension containing 4×10^3 cells was plated per well in a 96-well culture plate. The cells were cultured for 24, 48, and 72 h after which 10 μL CCK-8 solution from the CCK-8 assay kit (Dojindo, Tokyo, Japan) was added and incubated for 4 h, following the manufacturer's instructions. The absorbance was then determined in a microplate reader at an absorption wavelength of 450 nm. Each assay was done in triplicates.

Colony formation assay

Approximately 300 cells per well were introduced in a 6-well plate in triplicates. The cells were then grown for 9 days, and colonies were fixed in methanol and stained in crystal violet (0.1%) at room temperature for 1 h. Later, the plates were completely washed by submerging them in a water bath for 1 hour. Finally, the cell colonies were counted, and the percentage rate of colony formation was determined as colony number per 300 cells ×100, as described elsewhere (Rice *et al*., 2019). The assay was done in triplicates.

Transwell

Determination of cell migration was done using a transwell assay. Summarily, a 6.5 mm transwell chamber containing 8 μm pores (Corning Costar Corp., USA) was used. The ability of cells to migrate was investigated by re-suspension of the stably transfected cells (2×10^4 cells) in 200 μl of RMPI-1640 medium (serum-free) and eventually plating them in the top chamber. Later, 500 μl of the media supplemented with 10% fetal bovine serum was introduced into the lower well chamber. Cells were then incubated under chemotactic conditions for 24 h at 37°C. Cells were later stained in 1% crystal violet for 30 min, and cells on the upper surface of the membrane were eliminated using cotton swabs. Cells at the bottom of the membrane were then counted and imaged microscopically (Olympus Corp. Tokyo, Japan) in four random fields.

Flow cytometry test of apoptosis

The cells from a logarithmic phase were detached using 0.25% trypsin (without ethylene diamine tetraacetic acid) (PYG0107, Boster, Wuhan, China), washed in cold PBS, and collected in flow cytometry tubes. The cells were then centrifuged, and the supernatant was discarded. The Annexin-V-fluorescein isothiocyanate (FITC) Cell Apoptosis Detection Kit (K201-100, Biovision, USA) was applied to assess apoptosis following the manufacturer's instruction. The Annexin-V-FITC, propidium iodide (PI), and HEPES buffer solutions were appropriately prepared, and 1×10 cells were resuspended per 100 μL staining solution, incubated and 1 mL HEPES buffer was finally added. The apoptosis rate was finally detected using flow cytometry (BD Biosciences, Franklin Lakes, NJ, USA), and data were analyzed by CellQuest Pro (BD Biosciences, Franklin Lakes, NJ, USA). The experiment was repeated three times and data were averaged.

RNA stability analysis

In analyzing the half-life of CCND1 mRNA, HEK293T single clonal cell lines were treated using

10 μg/mL actinomycin D (Sigma) for transcription inhibition and were harvested at 0, 2, 4, 6, and 8 h. RT-qPCR was done to determine the decay in RNA abundance. Next, linear regression was then done between log values of the expression levels. Time points and the half-life were finally calculated.

Biotin RNA-pull down assay

The pull-down assay was done as described elsewhere (Barnes *et al.*, 2016). The biotinylated biotin-labeled MCF2L-AS1 and ELAVL1 (Bio-MCF2L-AS1/ELAVL1-AS/sense) (GeneCreate, Wuhan, China). (50 nM). Moreover, mutant plasmids (50 nM) were added to lysis buffer (500 μl, 0.5 M NaCl, 20 mM Tris-HCl, and 1 mM EDTA, pH 7.5) and incubated at 25°C with streptavidin-coated magnetic beads for 3 h. The cell pellets were then resuspended using the lysis buffer (1 ml/100 mg of cell pellet), and cell lysates were then incubated using the probe-coated beads. Lastly, the RNA mixture was finally eluted, and extraction was done for the northern blot using magnetic support, separating the beads from cell lysate. The supernatant was removed, and beads were washed using wash buffer (900 μl, 0.5% SDS, 2X SSC). Digoxin-labeled probes were prepared using the DIG Northern Starter kit (Roche Diagnostics GmbH) described earlier. Total RNA samples were resolved on 15% polyacrylamide-urea gels or 2% agarose and transferred to Hybond-N+ membranes (Amersham; Cytiva). The membranes were then dried, cross-linked by UV radiation, and hybridized using digoxin-labeled miR-140-5p probes at 42°C or 65°C overnight; the digoxin-labeled U6 probes were utilized as controls. The blot was visualized on a ChemiDoc XRS system (Bio-Rad Laboratories, Inc.).

RNA immunoprecipitation (RIP)

Approximately 1.7×10^6 cells were plated in a 10 cm dish and cultured for 48 h. Cells were then washed twice using chilled PBS, collected using a cell scraper into ice-cold PBS, and centrifuged at $500\times g$ for 5 min at 4°C. The pellets were resuspended using RIP lysis buffer (2 mL, 50 mM Tris/HCl, 300 mM NaCl, pH 7.4, 30 mM EDTA and 0.5% Triton X-100) supplement containing a cocktail of protease inhibitor and 200 U/ml RNaseOUT Recombinant Ribonuclease Inhibitor (Thermo Fisher) and incubated for 10 min on ice. The lysate was passed through a small needle severally and centrifuged for 15 min at $20\,000\times g$ and 4°C. Later, a supernatant (80 μL) was saved as input (10%) for the extraction of RNA, and another supernatant (80 μL) was set aside for analysis of protein. Dynabeads Protein G (50 μL) (Thermo Fisher) was washed twice using RIP lysis buffer (0.7 mL) and resuspended with RIP lysis buffer (150 μL). Next, rabbit anti-FMRP polyclonal antibody (10 μg) (Abcam, ab17722) or control normal rabbit IgG (10 μg) (Cell Signaling Technology) was added to the resuspended magnetic beads. The mixture was continuously centrifuged for 30 min at room temperature. The beads-antibody complex was washed four times using RIP lysis buffer (0.7 mL), mixed with cleared cell lysate (0.8 mL), and continuously centrifuged at 4°C for 3 h. The tubes were briefly centrifuged and placed on a magnetic separator. The supernatant (80 μL) was set aside as flow-through (10%) for protein analysis; beads were collected and washed (five times) at 4°C with RIP lysis buffer (0.7 mL) and resuspended with RIP lysis buffer (0.5 mL). Later, some mixture (50 μL) was saved as IP (10%) for analysis while 90% of the beads were transferred to a new tube, collected and resuspended using proteinase K digestion solution (150 μL), 15 μL of SDS (10%) and proteinase K (10 μL) (20 mg/ml; Thermo Scientific)]. In parallel, nuclease-free water (25 μL), 10% SDS (15 μL), and proteinase K (10 μL) were added to the input sample thawed on ice. Digestion of Proteinase K was done for 30 min at 55°C with shaking at 1200 rpm. The tubes were then briefly centrifuged and placed on a magnetic separator. The supernatant was transferred into a Phase Lock Gel Heavy tube, and NT2 buffer (250 μL) was added, followed by phenol:chloroform: isoamyl alcohol (400 μL) (Sigma-Aldrich). Tubes vortexing was done for 10 s and rotated for 10 min at $15000\times g$ and 4°C. The aqueous phase (400 μL) was transferred into a new tube. Recovering RNA from the aqueous phase was done by ethanol precipitation (overnight) with Pellet Paint Co-Precipitant (Millipore) according to the manufacturer's instructions. Purified input and immune-precipitated RNA were used in RT-qPCR. Additionally, input, IP, and flow-through samples were analyzed using SDS-PAGE and western blotting.

Chromatin immunoprecipitation (ChIP)

ChIP assays were done by Magna ChIP Kit (Millipore, Bedford, MA, USA) according to the manufacturer's instructions. The cells were treated with formaldehyde to generate DNA-protein cross-links. Cells were then lysed by sonication to generate 200–300 bp chromatin fragments. Finally, the cell lysates were immune-precipitated with an E2F1 specific antibody (Millipore) or IgG as a control for immunoprecipitation. After recovering the precipitated chromatin DNA, RT-qPCR analysis was performed.

The luciferase activity assay

The JASPAR (https://jaspa r.ger0eg.net/) online database was used to predict the latent transcription factor E2F1 binding motif in the promoter region of MCF2L-AS1. The various sequence of fragments was synthesized and then inserted into the pGL3-basic vector (Promega, Madison, WI, USA). Luciferase reporter experiment was done by seeding HEK293T cells (3.5×10^4 per well) into 48 well plates and transfected with the various plasmids (100 ng/well) using Lipofectamine 3000 transfection reagent (Invitrogen) as per the manufacturer's guidelines. Cells were then harvested 48 h post-transfection. Quantification of relative luciferase units was finally done using Dual-Luciferase® Reporter Assays (Promega, Fitchburg, WI, USA) following the manufacturer's guidelines on a GLOMAX 20/20 luminometer (Promega, Fitchburg, WI, USA).

Immunohistochemistry

The excised tumor tissues were fixed using PFA, embedding in paraffin, and the paraffin sections were routinely marked. After dewaxing and dehydration of the sections, extraction of the antigens was done by heating in a citric acid buffer solution, and the samples were incubated with the primary and secondary antibodies of Ki67 (1:1000, ab16667, Abcam). Finally, the samples were sealed with neutral glue. The prepared sections were Observed and photographed under a microscope (Nikon, Tokyo, Japan).

TdT-mediated dUTP-biotin nick end-labeling (TUNEL) staining

After dewaxing of paraffin sections with xylene and hydration with gradient ethanol, the samples were treated with proteinase K. Then, after incubation of the sections in 3% H_2O_2 and 0.1% TritonX-100 and biotinylation, the sections were stained with Diaminobenzidine and hematoxylin following the TUNEL kit instructions (Roche, USA). After dehydration with gradient ethanol, the sections were treated with xylene and sealed with neutral resin. The samples were finally observed and photographed under a microscope (Nikon).

RT-qPCR

Total RNA extraction was done using the TRIzol reagent (Invitrogen). The RNA samples' concentration and purity were then determined in a spectrophotometer NanoDrop2000 (Thermo Fisher Scientific, USA. High-capacity cDNA reverse transcription kit (Thermo Fisher Scientific, Vilnius, Lithuania) was applied for the synthesis of cDNA, with ABI 7900 system (Applied Biosystems, CA, USA) and SYBR Green kit (TaKaRa Biotechnology, Dalian, China) for real-time quantitative PCR. Calculation of the relative expression of RNA was done using the $2^{-\Delta\Delta CT}$ method. GAPDH was considered a loading control. The PCR primers were designed and synthesized by Beijing Kangwei Century Biotechnology Co., Ltd. The experiment was repeated three times, and the average was obtained. The primer sequences were as follows:

MCF2L-AS1: (F)5'-CCCAAAACCGCAGCTATCCT-3',
(R) 5'-TAAGGGGGAGTACTGCGTCA-3';
CCND1: (F) 5'-CGTGGCCTCTAAGATGAAGG-3',
(R) 5'-CTGGCATTTTGGAGAGGAAG-3';
ELAVL1: (F)5'-AGCTACGAATCTCCGACCAC-3',
(R) 5'-CGTTATCCCATGTGTCGAAGAA-3';
E2F1 (F) 5'-ACGCTATGAGACCTCACTGAA-3',
(R) 5'-TCCTGGGTCAACCCCTCAAG-3';
GAPDH: (F)5'-GGAGCGAGATCCCTCCAAAAT-3',
(R) 5'-GGCTGTTGTCATACTTCTCATGG-3'.

Western blot

Total protein was extracted from tissues and cells after transfection. Radio-Immunoprecipitation assay buffer (Sigma-Aldrich, Merck) was used for the lysis of cells. The protein concentration was measured via the bicinchoninic acid kit (Pierce, USA). The extracted protein samples were diluted in loading buffer and denatured by boiling. The protein was then separated using 10% sulfate-polyacrylamide gel electrophoresis. The electro-blot was later transferred onto a Polyvinylidene fluoride membrane (Millipore, Burlington, MA, USA) and blocked with 5% skim milk containing 0.1% Tween 20 tris buffered saline. The membrane was then incubated with anti-CCND1 (ab16663, 1:200), anti-ELAVL1 (ab2000342), anti-Ki67 (ab21700), anti-Bax (ab32503) (all 1:1000), anti-Bcl-2 (ab182858, 1:2000), and anti-cleaved caspase 3 (ab32042, 1:500) at 4°C overnight. The samples were then incubated with the corresponding horseradish peroxidase-conjugated secondary antibody (ab109489, 1:1000). A chemiluminescence reagent (Millipore, Burlington) was employed to observe the protein bands. ImageJ software (NIH, Bethesda, MD, USA) was used for the band analysis, and GAPDH (ab8245, 1:500) was used as a loading control.

Data analysis

Statistical analysis of data was done using SPSS 19.0 (IBM, Chicago, IL, USA). The data were presented as mean ± standard deviation. Each experiment was repeated at least three times. Comparison of the differences between the two groups was made *via* Student's *t*-test while the difference in multiple groups was determined using done one-way analysis of variance. Estimation of the correlation between the two genes was investigated by Pearson correlation analysis. $P<0.05$ was considered statistically significant.

RESULTS

LncRNA MCF2L-AS1 is up-regulated in Gefitinib-resistant NSCLC patients

To understand the association of lncRNA MCF2L-AS1 and gefitinib-resistance in NSCLC, RT-qPCR was

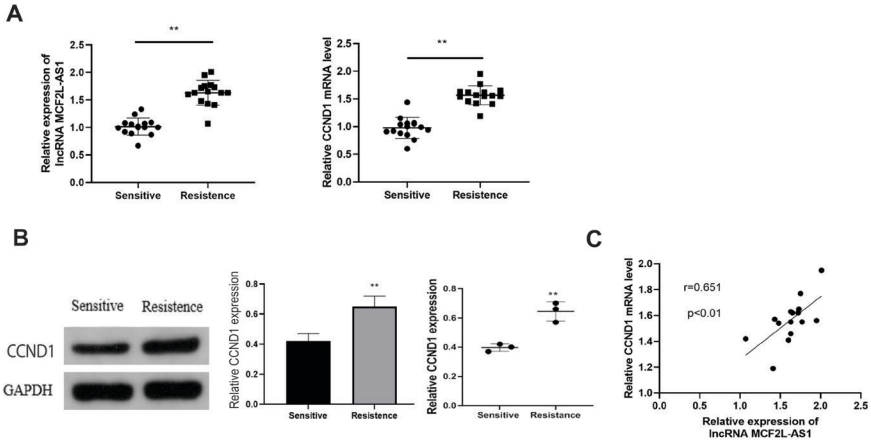

Figure 1. LncRNA MCF2L-AS1 is elevated in Gefitinib-resistant NSCLC patients.
(**A**) RT-qPCR detection of lncRNA MCF2L-AS1 and CCND1 mRNA expressions in Gefitinib-sensitive and Gefitinib-resistant NSCLC patients' tissues; (**B**) WB detection of CCND1 in Gefitinib-sensitive and resistant NSCLC tissues; (**C**) determination of the correlation of lncRNA MCF2L-AS1 and CCND1 in NSCLC tissues. The data was repeated three times (N=3); n=15, *$P<0.05$, **$P<0.01$, ***$P<0.001$.

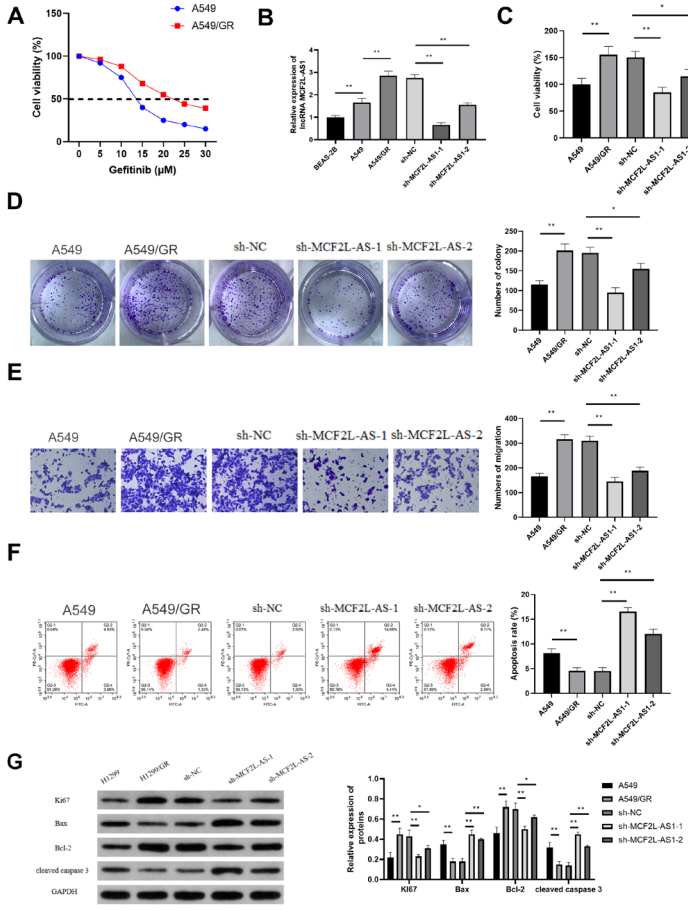

Figure 2. Knockdown of lncRNA MCF2L-AS1 inhibits Gefitinib resistance in NSCLC
(**A**) CCK-8 detection of cell viability in parental A549 and A549/GR cells after treatment with increasing doses of Gefitinib; (**B**) RT-qPCR detection of lncRNA MCF2L-AS1 in normal human BEAS-2B, A549 and A549/GR and A549/GR cells transfected with sh-MCF2L-AS1-1, sh-MCF2L-AS1-2 OR sh-NC; (**C–D**) CCK-8 and colony formation detection of cell proliferation; (**E**) Flow cytometry; (**F**) WB detection of apoptosis proteins including Bax, Bcl-2, cleaved caspase 3, and Ki67 genes. N=3, **P*<0.05, ***P*<0.01, ****P*<0.001.

used to determine the expression of lncRNA MCF2L-AS1 in Gefitinib sensitive and Gefitinib resistant tissues. The results confirmed an elevated lncRNA MCF2L-AS1 mRNA expression in the Gefitinib-resistant compared to the Gefitinib sensitive tissues. Further RT-qPCR results also confirmed significantly increased CCND1 mRNA expression in the Gefitinib-resistant than in the Gefitinib-sensitive NSCLC tissues (Fig. 1A). Investigation of ELAVL1 expression through western blot confirmed significantly increased ELAVL1 protein in the Gefitinib resistant tissues compared to the sensitive group (Fig. 1B). Finally, the Pearson correlation analysis determined the correlation between CCND1 and lncRNA MCF2L-AS1. The results confirmed a positive correlation between lncRNA MCF2L-AS1 and CCND1 (Fig. 1C) ($P<0.01$). These results confirmed that lncRNA MCF2L-AS1 was up-regulated in Gefitinib-resistant NSCLC patients.

Knockdown of lncRNA MCF2L-AS1 inhibits Gefitinib resistance in NSCLC

In studying the effect of lncRNA MCF2L-AS1 on gefitinib resistance in LC, A549 cells were treated with increasing concentrations of Gefitinib to achieve clones of NSCLC Gefitinib-resistant cells (A549/GR). The cell viability determination confirmed that the IC50 value of Gefitinib-resistant NSCLC cells (A549/GR) was significantly increased than in the parent cells (A549) (Fig. 2A) ($P<0.01$). Next, RT-qPCR was used to assess the lncRNA MCF2L-AS1 expression in BEAS-2B, A549, A549/GR, and the cells transfected with sh-MCF2L-AS1-1, sh-MCF2L-AS1-2, or sh-NC. The results confirmed that lncRNA MCF2L-AS1 mRNA expression was significantly increased in A549/GR cells compared to parental and BEAS-2B cells (Fig. 2B) ($P<0.01$). Next, a CCK-8 assay was carried out to determine the cell viability after the knockdown of MCF2L-AS1-1. The results confirmed a significantly increased cell growth in A549/GR compared to A549 cells. However, the cell viability was significantly reduced following the knockdown of MCF2L-AS1-1 in the sh-MCF2L-AS1-1 and sh-MCF2L-AS1-2-transfected cells (Fig. 2C). The colony formation assay also confirmed increased colonies in the A549/GR cells compared to the parental 549 cells. However, the colony numbers were significantly reduced in the sh-MCF2L-AS1-1 and sh-MCF2L-AS1-2 compared to the sh-NC groups (Fig. 2D). Migration was also studied by transwell assay. The results confirmed significantly increased migration in the A549/GR cells compared to the parental A549 cells. However, the migration was significantly reduced in the sh-MCF2L-AS1-1 and sh-MCF2L-AS1-2 compared to the sh-NC group (Fig. 2E). Investigation of apoptosis through flow cytometry confirmed significantly reduced apoptosis in the A549/GR than the parental cells. After the knockdown, apoptosis was significantly increased in the sh-MCF2L-AS1-1 and sh-MCF2L-AS1-2

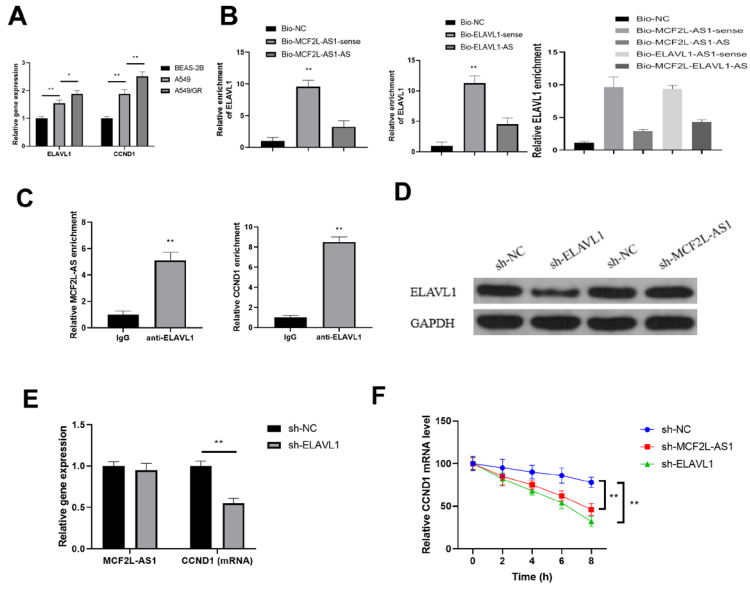

Figure 3. LncRNA MCF2L-AS1 enhances CCND1 mRNA stability through combining with ELAVL1
(**A**) RT-qPCR detection of ELAVL1 and CCND1 in BEAS-2B, A549, and A549/GR cells; (**B–C**). RNA pull-down and RIP separate verification of the modulatory effects among lncRNA MCF2L-AS1, ELAVL1, and CCND1; (**D**) WB detection of ELAVL1 in A549/GR cells transfected with sh-ELAVL1, sh-MCF2L-AS1, and sh-NC; E-F. RT-qPCR detection of MCF2L-AS1, CCND1, and CCND1 mRNA stability in A549/GR cells transfected with sh-MCF2L-AS1, sh-ELAVL1, or sh-NC. N=3, *P<0.05, **P<0.01, ***P<0.001.

compared to the sh-NC cells (Fig. 2F) (P<0.01). Finally, a western blot was used to study the expressions of various apoptosis markers. The observations confirmed significantly increased expressions of the proliferation marker protein Ki67 and the anti-apoptotic protein Bcl-2 in the Gefitinib-resistant cells, while the pro-apoptosis proteins (Bax and cleaved caspase 3) were significantly reduced. These results were, however, reversed after knocking down MCF2L-AS1 (Fig. 2F) (P<0.01). According to these observations, knockdown of lncRNA MCF2L-AS1 down-regulated Gefitinib resistance in NSCLC.

LncRNA MCF2L-AS1 enhances CCND1 mRNA stability through combining with ELAVL1

To investigate the mechanisms and association of ELAVL1 and CCND1, RT-qPCR was used to determine ELAVL1 and CCND1 expression in BEAS-2B, A549, and A549/GR cells. The observations confirmed significantly increased ELAVL1 and CCND1 mRNA expressions in A549 and A549/GR cells compared to the BEAS-2B cells (Fig. 3A). Assessment of the association of ELAVL1 with MCF2L-AS1 confirmed an interaction between lncRNA MCF2L-AS1 and ELAVL1 in Gefitinib-resistant LC cells (Fig. 3B). There was also a significantly increased enrichment of MCF2L-AS1 and CCND1 in the ELAVL1 than the control IgG (Fig. 3C) (P<0.01). Western blot was then used to determine the level of ELAVL1 in the A549/GR cells transfected with sh-ELAVL1, sh-NC, sh-MCF2L-AS1, and sh-NC. The results confirmed significantly reduced ELAVL1 expression in sh-ELAVL1 transfected cells compared to sh-NC cells. However, ELAVL1 expression was significantly increased in the sh-MCF2L-AS1 compared to its sh-NC counterpart (Fig. 3D) (P<0.01). Meanwhile, after ELAVL1 silencing, MCF2L-AS1 mRNA expression was not significantly changed, while CCND1 was greatly reduced compared to the sh-NC (Fig. 3E) (P<0.01). Finally, the cells were treated with actinomycin D (transcription inhibitor) to observe the impacts of MCF2L-AS1 and ELAVL1 on the stability of CCND1 mRNA. The results confirmed that knockdown of MCF2L-AS and ELAVL1 independently significantly reduced the half-life of CCND1 mRNA than the sh-NC (Fig. 3F) (P<0.01). In summary, the results clarified that lncRNA MCF2L-AS1 motivated CCND1 mRNA stability in LC Gefitinib-resistant cells via combining with ELAVL1.

Strengthening CCND1 reverses the effects of the knockdown of lncRNA MCF2L-AS1 on Gefitinib resistance in NSCLC

To study whether lncRNA MCF2L-AS1 functions by controlling CCND1 in Gefitinib resistance to LC, a functional rescue experiment was carried out by transfecting the A549/GR cells with the sh-MCF2L-AS1 + Oe-NC, sh-MCF2L-AS1+Oe-CCND1, or sh-NC plasmids. Western blot was then done to determine the CCND1 expression. The results confirmed significantly reduced CCND1 proteins sh-MCF2L-AS1 + Oe-NC but increased levels in the sh-MCF2L-AS1 + Oe-CCND1 group (Fig. 4A) (P<0.01). Cell viability studies confirmed significantly reduced proliferation in the sh-MCF2L-AS1 + Oe-NC group, which was, however, reversed in sh-MCF2L-AS1 + Oe-CCND1 cells (Fig. 4B) (P<0.01). Additionally, cell colonies were significantly reduced in the sh-MCF2L-AS1 + Oe-NC but increased in the sh-MCF2L-AS1 + Oe-CCND1 (Fig. 4C) (P<0.01). The transwell assays also confirmed significantly reduced migration in the sh-MCF2L-AS1 + Oe-NC, which was later increased in the sh-MCF2L-AS1 + Oe-CCND1(Fig. 4D) (P<0.01). The flow cytometry analysis confirmed significantly increased apoptosis following the transfection of A549/GR cells with sh-MCF2L-AS1 + Oe-NC plasmid. However, the apoptosis was remarkably down-regulated in the sh-MCF2L-AS1 + Oe-CCND1 cells (Fig. 4E) (P<0.01). Finally, the western blot analysis significantly reduced Ki67 and Bcl-2 but increased Bax and cleaved caspase 3 in the sh-MCF2L-AS1 + Oe-CCND1 cells. Nevertheless, Ki67 and Bcl-2 were significantly up-regulated, but Bax and cleaved caspase 3 were down-regulated in the sh-MCF2L-AS1 + Oe-CCND1 cells (Fig. 4F)

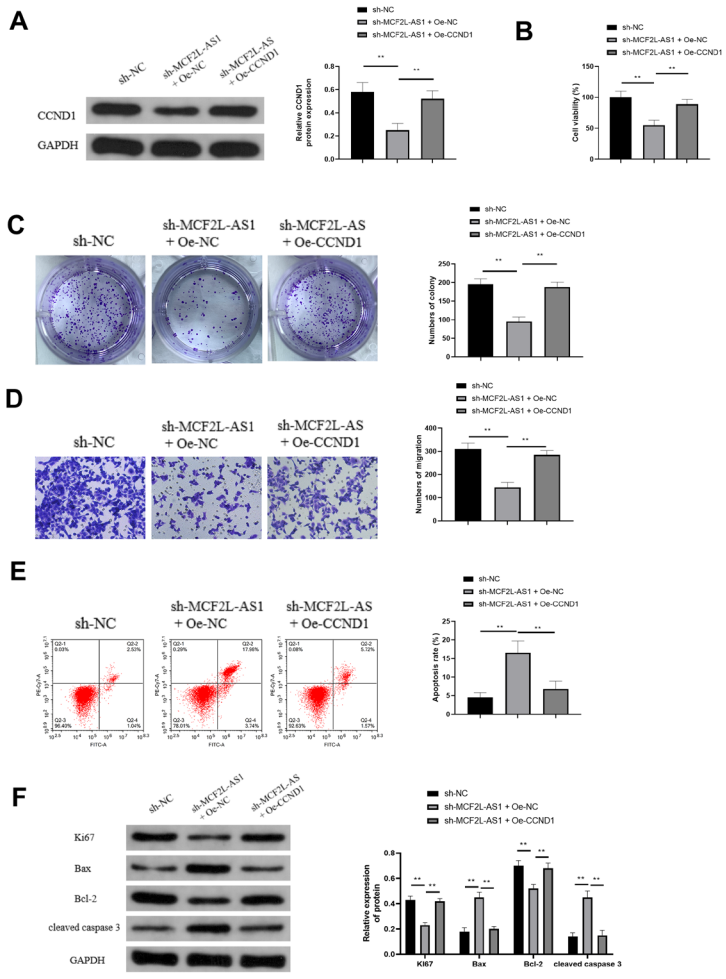

Figure 4. Strengthening CCND1 reverses the effects of the knockdown of lncRNA MCF2L-AS1 on Gefitinib resistance in NSCLC
(**A**) WB detection of CCND1 in A549/GR cells transfected with sh-MCF2L-AS1+oe-NC, sh-MMCF2L-AS1+oe-CCND1 or sh-NC; (**B–C**) CCK-8 and colony formation detection of cell proliferation; (**D**) Flow cytometry; (**F**) WB detection of cell apoptosis proteins including Ki67, Bax, Bcl-2, and cleaved caspase 3. N = 3, **P*<0.05, ***P*<0.01, ****P*<0.001.

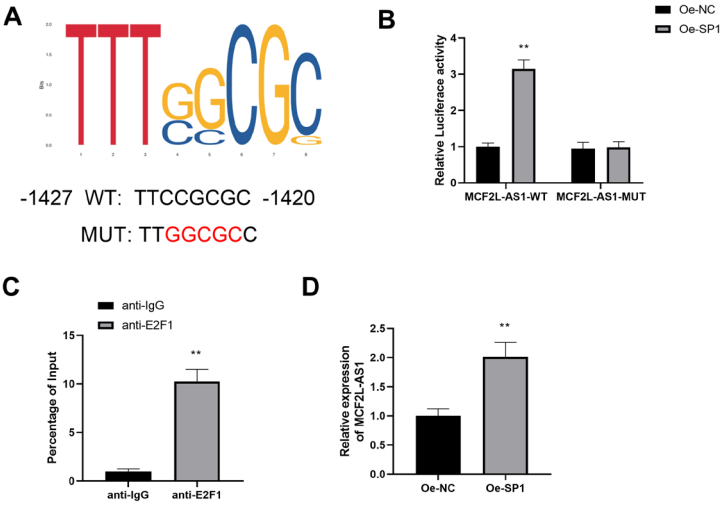

Figure 5. E2F1 transcription modulates lncRNA MCF2L-AS1
(**A**) JASPAR online prediction of the binding site of transcription factor E2F1 and MCF2L-AS1 promoter; (**B–C**) The luciferase activity and ChIP assays verification of the interaction between E2F1 and MCF2L-AS1; D. RT-qPCR detection of MCF2L-AS1. N=3, **P*<0.05, ***P*<0.01, ****P*<0.001.

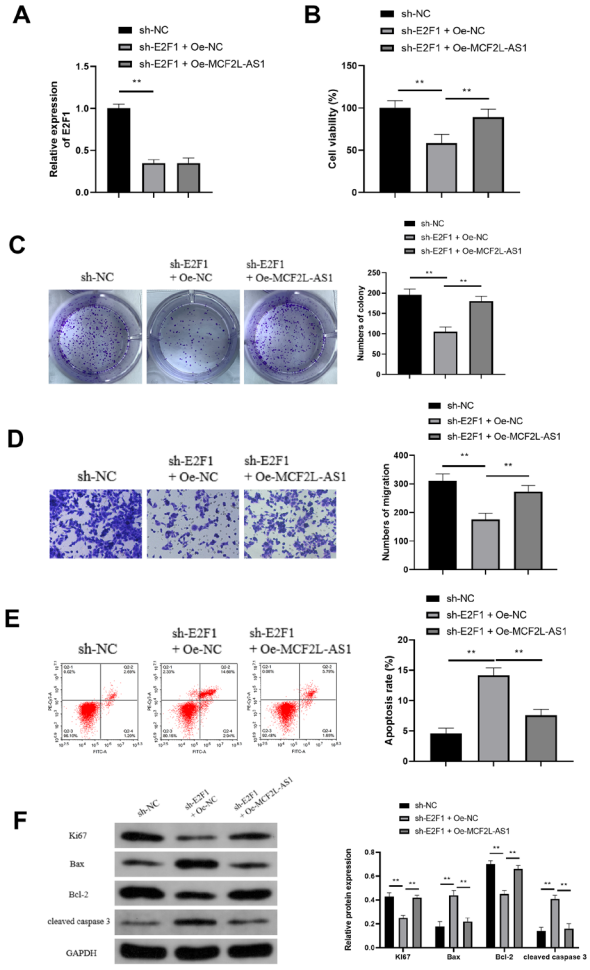

Figure 6. E2F1 transcription elevates lncRNA MCF2L-AS1 to modulate Gefitinib resistance in NSCLC
(**A**) RT-qPCR detection of E2F1 in A549/GR cells transfected with sh-E2F1+oe-NC, sh-E2F1+oe-MCF2L-AS1 or sh-NC; (**B–C**) CCK-8 and colony formation detection of cell proliferation; (**D–E**) Flow cytometry and WB detection of cell apoptosis. N=3, **P*<0.05, ***P*<0.01, ****P*<0.001.

(*P*<0.01). The results confirmed that CCND1 overexpression weakened the impact of lncRNA MCF2L-AS1 knockdown on the resistance of Gefitinib to NSCLC.

E2F1 transcription modulates lncRNA MCF2L-AS1

To further study the upstream modulatory mechanism of lncRNA MCF2L-AS1, the JASPAR bioinformatics tool was used to predict a possible binding. The results confirmed that the transcription factor E2F1 and MCF2L-AS1 promoter region had latent binding sites (Fig. 5A). The dual-luciferase assay confirmed significantly increased luciferase activity in the MCF2L-AS1-WT groups transfected with the transcription factor specificity protein 1 (SP1) (oe-SP1) compared to the oe-NC-transfected group. However, there was no significant change in the MCF2L-AS1-MUT group (Fig. 5B). The ChIP analysis also confirmed that the transcription factor E2F1 interacted with the MCF2L-AS1 promoter (Fig. 5C) (*P*<0.01). Finally, RT-qPCR was used to determine MCF2L-AS1 expression after the elevation of E2F1. The results confirmed a significantly reduced MCF2L-AS1 expression in the oe-SP1 compared to the oe-NC group (Fig. 5D) (*P*<0.01). These observations confirmed that E2F1 transcriptionally up-regulated the MCF2L-AS1 expression.

E2F1 transcription elevates lncRNA MCF2L-AS1 to modulate Gefitinib resistance in NSCLC

For investigating whether E2F1 affected Gefitinib resistance to NSCLC via modulating lncRNA MCF2L-AS1, A549/GR cells were transfected with sh-E2F1 + Oe-NC, sh-E2F1 + Oe-MCF2L-AS1, or sh-NC plasmids. RT-qPCR was then used to determine E2F1 expression. The observations confirmed that MCF2L-AS1 overexpression has no impact on E2F1 mRNA expression (Fig. 6A) (*P*<0.01). CCK-8 analysis showed significantly reduced A549/GR cell proliferation following the silencing of E2F1 but enhanced growth after MCF2L-AS1 overexpression (Fig. 6B) (*P*<0.01). The colony formation assay and transwell results also confirmed significantly reduced colonies and migration in the sh-E2F1 + Oe-NC but increased in the sh-E2F1 + Oe-MCF2L- AS1 cells(Fig. 6C–D) (*P*<0.01). The flow cytometry analysis confirmed significantly increased apoptosis in sh-E2F1 + Oe-NC but was remarkably reduced in the sh-E2F1 + Oe-MCF2L-AS1 cells (Fig. 6E) (*P*<0.01). Western blot analysis confirmed significantly reduced Ki67 and Bcl-2 but increased Bax and cleaved caspase 3 expressions in the sh-E2F1+oe-NC group. However, the expressions of these proteins were reversed in the sh-E2F1 + Oe-MCF2L-AS1 cells (Fig. 6F). Put together, these observations

confirmed that E2F1 transcription elevated lncRNA MCF2L-AS1 to modulate Gefitinib resistance in NSCLC.

DISCUSSION

Gefitinib is a chemotherapeutic drug that disrupts EGFR-mediated signaling in the targeted cells. Gefitinib has been regarded as the standard first-line therapy for advanced NSCLC patients with EGFR-activating mutations. In over 50% of the cases of Gefitinib treatment failure, T790M mutation in EGFR is always implicated (Wang *et al*., 2020). Recent findings have proven that lncRNAs play crucial functions in malignant tumors pathogenesis by controlling genes associated with cell proliferation, apoptosis, metastasis, and radio-or chemoresistance (Lin *et al*., 2018). Nevertheless, the mechanisms involved in lncRNA-initiated Gefitinib resistance to therapy are yet to be clarified.

In the current investigation, we constructed a Gefitinib-resistant cell line referred to as A549/GR to assess the lncRNA MCF2L-AS1 and CCND1-mediated mechanisms of resistance to Gefitinib. This cell line has been associated with resistance to Gefitinib (Ma *et al*., 2017). We discovered that CCND1 is increased in Gefitinib-resistant NSCLC patients and is positively linked with lncRNA MCF2L-AS1. Simultaneously, both ELAVL1 and CCND1 were enhanced in Gefitinib-resistant cells. It was confirmed that lncRNA MCF2L-AS1 contributes to CCND1 mRNA stability *via* combining with ELAVL1. Meanwhile, it was also verified that E2F1 transcriptionally up-regulates lncRNA MCF2L-AS1. Mechanically, it was originally reported that E2F1-transcriptionally modulated lncRNA MCF2L-AS1 elevated CCND1 mRNA stability through combining with ELAVL1 to motivate Gefitinib resistance in NSCLC.

The role of lncRNA in the progression of tumors and the establishment of drug resistance has been widely reported. LncRNA MCF2L-AS1 has been reported to be enhanced in LC tissues and cells and drives NSCLC stem cell-like characteristics *via* inhibiting miR-873-5p.

Additionally, lncRNA MCF2L-AS1 has been associated with colorectal cancer cells' progression and resistance to Oxaliplatin CRC's presence and progression (Cai *et al*., 2021). Nevertheless, there are currently no reports on the character and mechanism of lncRNA MCF2L-AS1 in NSCLC and Gefitinib resistance. The present research originally reports that lncRNA MCF2L-AS1 is up-regulated in gefitinib-resistant NSCLC patients and gefitinib-resistant cells and drives Gefitinib resistance in NSCLC *in vivo* and *in vitro*.

Previous studies have elucidated that lncRNA control downstream gene expression via combining with RBP to function in various illnesses. For instance, lncRNA OIP5-AS1 contributes to the stability of MEF2C mRNA via combining with HUR to accelerate myogenesis (Yang *et al*., 2020). Additionally, silencing SCAMP1-TV2 elevates the degradation of INSM1 mRNA *via* interacting with PUM2, thereby inhibiting the malignant biological behavior of BC cells (Tao *et al*., 2020). Here, we report an increased ELAVL1 expression in Gefitinib-resistant cells. This finding is in agreement with a previous report that associated NSCLC progression with the binding of HuR (ELAVL1) to CDC6 (Zhang *et al*., 2020).

Cell cycle progression is determined by a well-tuned cascade of signal transduction, whereby D-type cyclins have a crucial role. Human cyclin D proteins encode three D-type cyclins, including cyclin D1 (CCND1), cyclin D2 (CCND2), and cyclin D3 (CCND3) (Zhang *et al*., 2021). Each of these genes may interact with other proteins, hence activating cyclin-dependent kinase 4/6, which eventually phosphorylates retinoblastoma (Rb) protein and thus induces the transition of the G1/S phase cell cycle. In this work, CCND1 was shown to co-operate with lncRNA MCF2L-AS1 to induce Gefitinib resistance in NSCLC. This finding confirms the importance of CCND1 in NSCLC as was also previously reported where CCND1 was elevated and associated with the promotion of carcinogenesis, progression of the cell cycle, drug resistance, and metastasis in NSCLC (Liu *et al*., 2020).

In conclusion, this research fundamentally highlights the molecular mechanism of the lncRNA MCF2L-AS1 in inducing the growth and resistance of Gefitinib to NSCLC. The results manifest that lncRNA MCF2L-AS1, as an oncogene of NSCLC, controls CCDN1 *via* ELAVL1 to drive the growth of NSCLC cells and Gefitinib resistance. The novel findings of this investigation give a basis for targeting lncRNA MCF2L-AS1 and its downstream molecular axis as a possible alternative for developing effective and sensitive drug therapy against NSCLC.

Declarations

Declaration of Conflicting Interests. The author(s) declared no potential conflicts of interest with respect to the research, authorship, and/or publication of this article.

REFERENCES

Ajani JA, Song S, Hochster HS, Steinberg IB (2015) Cancer stem cells: the promise and the potential. *Seminars Oncol* **42** (Suppl 1): S3–S17. https://doi.org/10.1053/j.seminoncol.2015.01.001

Cai M, Hu W, Huang C, Zhou C, Li J, Chen Y, Yu Y (2021) lncRNA MCF2L-AS1/miR-105/IL-1β axis regulates colorectal cancer cell oxaliplatin resistance. *Cancer Manag Res* **13**: 8685–8694. https://doi.org/10.2147/cmar.S313905

Chai W, Liu R, Li F, Zhang Z, Lei B (2021) Long noncoding RNA TSLNC8 enhances pancreatic cancer aggressiveness by regulating CTNNB1 expression via association with HuR. *Hum Cell* **34**: 165–176. https://doi.org/10.1007/s13577-020-00429-4

Chen X, Wang Z, Tong F, Dong X, Wu G, Zhang R (2020) lncRNA UCA1 promotes gefitinib resistance as a ceRNA to target FOSL2 by sponging miR-143 in non-small cell lung cancer. *Mol Therap Nucleic Acids* **19**: 643–653. https://doi.org/10.1016/j.omtn.2019.10.047

Huang FK, Zheng CY, Huang LK, Lin CQ, Zhou JF, Wang JX (2021) Long non-coding RNA MCF2L-AS1 promotes the aggressiveness of colorectal cancer by sponging miR-874-3p and thereby up-regulating CCNE1. *J Gene Med* **23**: e3285. https://doi.org/10.1002/jgm.3285

Kwon T, Rho JK, Lee JC, Park YH, Shin HJ, Cho S, Kang YK, Kim BY, Yoon DY, Yu DY (2015) An important role for peroxiredoxin II in survival of A549 lung cancer cells resistant to gefitinib. *Exp Mol Med* **47**: e165. https://doi.org/10.1038/emm.2015.24

Lei Y, Guo W, Chen B, Chen L, Gong J, Li W (2018) Tumor-released lncRNA H19 promotes gefitinib resistance *via* packaging into exosomes in non-small cell lung cancer. *Oncol Rep* **40**: 3438–3446. https://doi.org/10.3892/or.2018.6762

Li S, Lin L (2021) Long noncoding RNA MCF2L-AS1 promotes the cancer stem cell-like traits in non-small cell lung cancer cells through regulating miR-873-5p level. *Environ Toxicol* **36**: 1457–1465. https://doi.org/10.1002/tox.23142

Lin C, Yang L (2018) Long Noncoding RNA in cancer: wiring signaling circuitry. *Trends Cell Biol* **28**: 287–301. https://doi.org/10.1016/j.tcb.2017.11.008

Liu B, Chen D, Chen S, Saber A, Haisma H (2020) Transcriptional activation of cyclin D1 *via* HER2/HER3 contributes to EGFR-TKI resistance in lung cancer. *Biochem Pharmacol* **178**: 114095. https://doi.org/10.1016/j.bcp.2020.114095

Ma W, Kang Y, Ning L, Tan J, Wang H, Ying Y (2017) Identification of microRNAs involved in gefitinib resistance of non-small-cell lung cancer through the insulin-like growth factor receptor 1 signaling pathway. *Exp Therap Med* **14**: 2853–2862. https://doi.org/10.3892/etm.2017.4847

Ni ZZ, He JK, Tang X, Tao Z, Zhang Y, Xie B (2020) Identification of ELAVL1 gene and miRNA-139-3p involved in the aggressiveness of NSCLC. *Eur Rev Med Pharmacol Sci* **24**: 9453–9464. https://doi.org/10.26355/eurrev_202009_23030

Rho JK, Choi YJ, Lee JK, Ryoo BY, Na II, Yang SH, Kim CH, Lee JC (2009)Epithelial to mesenchymal transition derived from repeated exposure to gefitinib determines the sensitivity to EGFR inhibitors in A549, a non-small cell lung cancer cell line. *Lung Cancer (Amsterdam, Netherlands)* **63**: 219–226. https://doi.org/10.1016/j.lungcan.2008.05.017

Rice MA, Hsu EC, Aslan M, Ghoochani A, Su A, Stoyanova T (2019) Loss of Notch1 activity inhibits prostate cancer growth and metastasis and sensitizes prostate cancer cells to antiandrogen therapies. *Mol Cancer Therap* **18**: 1230–1242. https://doi.org/10.1158/1535-7163.Mct-18-0804

Sana J, Faltejskova P, Svoboda M, Slaby O (2012) Novel classes of non-coding RNAs and cancer. *J Transl Med* **10**: 103. https://doi.org/10.1186/1479-5876-10-103

Sun HB, Han XL, Zhong M, Yu DJ (2020) Linc00703 suppresses non-small cell lung cancer progression by modulating CyclinD1/CDK4 expression. *Eur Rev Med Pharmacol Sci* **24**: 6131–6138. https://doi.org/10.26355/eurrev_202006_21508

Tao W, Ma J, Zheng J, Liu X, Liu Y, Ruan X, Shen S, Shao L, Chen J, Xue Y (2020) Silencing SCAMP1-TV2 inhibited the malignant biological behaviors of breast cancer cells by interaction with PUM2 to facilitate INSM1 mRNA degradation. *Front Oncol* **10**: 613. https://doi.org/10.3389/fonc.2020.00613

Wang H, Lu B, Ren S, Wu F, Wang X, Yan C, Wang Z (2020) Long noncoding RNA LINC01116 contributes to gefitinib resistance in non-small cell lung cancer through regulating IFI44. *Mol Ther Nucleic Acids* **19**: 218–227. https://doi.org/10.1016/j.omtn.2019.10.039

Wu C, Zhu XT, Xia L, Wang L, Yu W, Guo Q, Zhao M, Lou J (2020) High expression of long noncoding RNA PCNA-AS1 promotes non-small-cell lung cancer cell proliferation and oncogenic activity *via* upregulating CCND1. *J Cancer* **11**: 1959–1967. https://doi.org/10.7150/jca.39087

Yang JH, Chang MW, Pandey PR, Tsitsipatis D, Yang X, Martindale JL, Munk R, De S, Abdelmohsen K, Gorospe M (2020) Interaction of OIP5-AS1 with MEF2C mRNA promotes myogenic gene expression. *Nucleic Acids Res* **48**: 12943–12956. https://doi.org/10.1093/nar/gkaa1151

Zhang T, Beeharry MK, Zheng Y, Wang Z, Li J, Zhu Z, Li C (2021) Long noncoding RNA SNHG12 promotes gastric cancer proliferation by binding to HuR and stabilizing YWHAZ expression through the AKT/GSK-3β pathway. *Front Oncol* **11**: 645832. https://doi.org/10.3389/fonc.2021.645832

Zhang X, Lian T, Fan W, Zhang G, Chen Z, Gou X, Jha RK (2020) Long-noncoding RNA CASC9 promotes progression of non-small cell lung cancer by promoting the expression of CDC6 through binding to HuR. *Cancer Manag Res* **12**: 9033–9043. https://doi.org/10.2147/cmar.S268375

Zhang Z, Cui Z, Xie Z, Li C, Xu C, Guo X, Yu J, Chen T, Facchinetti F, Bohnenberger H, Leong TL, Xie Y, Mao X, Zhao J (2021) Deubiquitinase USP5 promotes non-small cell lung cancer cell proliferation by stabilizing cyclin D1. *Transl Lung Cancer Res* **10**: 3995–4011. https://doi.org/10.21037/tlcr-21-767

Zhang Z, Yang W, Li N, Chen X, Ma F, Yang J, Zhang Y, Chai X, Zhang B, Hou X, Luo S, Hua Y (2021) LncRNA MCF2L-AS1 aggravates proliferation, invasion and glycolysis of colorectal cancer cells *via* the crosstalk with miR-874-3p/FOXM1 signaling axis. *Carcinogenesis* **42**: 263–271. https://doi.org/10.1093/carcin/bgaa093